Complex Phase Behavior in Solvent-Free Nonionic Surfactants

Marc A. Hillmyer,* Frank S. Bates,* Kristoffer Almdal,
Kell Mortensen, Anthony J. Ryan, J. Patrick A. Fairclough

Unsolvated block copolymers and surfactant solutions are "soft materials" that share a common set of ordered microstructures. A set of polyethyleneoxide-polyethylethylene (PEO-PEE) block copolymers that are chemically similar to the well-known alkane-oxyethylene (C_nEO_m) nonionic surfactants was synthesized here. The general phase behavior in these materials resembles that of both higher molecular weight block copolymers and lower molecular weight nonionic surfactant solutions. Two of the block copolymers exhibited thermally induced order-order transitions and were studied in detail by small-angle scattering. The fundamental microstructural spacing was determined to be a crucial parameter in these transitions. Transitions from one ordered state to another occur only when the lattice spacing is nearly matched. These materials highlight the importance of epitaxy and molecular conformation in the phase transformations of soft material.

Amphiphilic molecules such as surfactants, phospholipids, and ionic soaps self-assemble into micelles in dilute aqueous solution because of the hydrophobic effect. As the concentration of the amphiphile increases, thermodynamically stable supramolecular aggregates form with a variety of ordered-state symmetries (*1*, *2*). Transitions between phases in these lyotropic liquid crystals (LCs) can be induced thermally or by changes in amphiphile concentration. The nature of these phase transitions has implications in cell membrane structure and function (*2*–*4*). Also, surfactant mesophases have been used as templates for polymerizations (*5*), synthesis of metal nanoparticles (*6*), and in the preparation of mesoporous ceramics (*7*, *8*). Although significant theoretical work has been done in the field of lyotropic LCs, our understanding is far from complete (*3*, *9*).

Block copolymer melts are a separate class of soft materials that spontaneously order below a critical temperature (*10*, *11*). Conformational freedom associated with a long flexible chain allows microstructures with curved interfaces to form. As the polymer chains become smaller, it is reasonable to assume that this feature will eventually be lost. What is observed in most monomeric thermotropic LCs is that they adopt layered (smectic) or nematic phases (*12*), unlike the topologically complex phases (such as bicontinuous cubic phases) observed in block copolymers. Clearly, lyotropic LCs and block copolymers are related through a common set of observed phases, a connection that has been made by us and by others (*3*, *9*, *13*, *14*). However, the theoretical approaches aimed at understanding the phase behavior and transformations in these complex materials are fundamentally different.

Block copolymer theories (*11*, *15*) generally deal with the limit of infinite molecular weight (MW), whereas lyotropic theories (*2*, *3*) must contend with binary (or greater) mixtures of components of relatively low MW. Block copolymer theories balance entropic loss associated with chain stretching against enthalpic penalties associated with segment-segment contact. Chain packing frustration, head-group interactions, and bilayer elastic bending energy are the most important contributors to theories of lyotropic LC.

We report here the bulk-phase behavior of a set of molecules that can be thought of as either large nonionic surfactants or small amphiphilic block copolymers. These molecules share certain general characteristics of both solvated nonionic surfactants and unsolvated block copolymers. These materials also show a feature that may lend fresh insight into the nature of phase transformations in soft materials. The design of these molecules was based on that of the well-known alkane-oxyethylene (C_nEO_m) nonionic surfactants (*9*, *16*, *17*).

Nonionic surfactants of this type exhibit mesomorphism at intermediate concentrations in water, but unlike block copolymers these small, amphiphilic molecules do not form ordered mesophases in the solvent-free state. Instead, they disorder above the crystalline melting temperature (T_m) because of the relatively large entropic contribution to the free energy associated with a low MW (*10*). To move to higher MW systems, we synthesized model polyethyleneoxide-polyethylethylene (PEO-PEE) block copolymers using anionic polymerization and catalytic hydrogenation (Fig. 1) (*18*). The chemical composition of these oxyethylene-alkane polymers is similar to that of the C_nEO_m nonionic surfactants, but the MWs are an order of magnitude greater (2.5 to 8.9 kg/mol) for the former, and the alkane block does not crystallize (*19*). Ten PEO-PEE block copolymers with PEO volume fractions ranging from 29 to 72% were synthesized in near quantitative yields and with low polydispersities ($\overline{M}_w/\overline{M}_n \cong 1.1$, where $\overline{M}_w$ and $\overline{M}_n$ are the weight average and number average molecular weights, respectively). All of the polymers form ordered microstructures above the T_m of the crystalline PEO block and melt into isotropic disordered liquids (DIS) at experimentally tractable temperatures (<275°C). The increase in the MW of these nonionic surfactants has led to the formation of ordered morphologies in the absence of water.

We used small-angle neutron and small-angle x-ray scattering (SANS and SAXS) to identify the following ordered state symmetries: semicrystalline lamellae (L_c), where the PEO block is crystalline; a normal lamellar structure (L) composed of amorphous blocks; a modified lamellar structure (ML) we believe to be topologically similar to the hexagonally perforated layered phase seen in block copolymers (*20*) or the randomly perforated lamellar phase observed in lyotropics (*21*); a bicontinuous cubic phase with $Ia\bar{3}d$ space group symmetry ($Q_{Ia\bar{3}d}$); and hexagonally packed cylinders (H). These four noncrystalline ordered morphologies are depicted in Fig. 2 (*22*). Even at these low MWs, ordered phases with curved interfaces were observed. Furthermore, features of the preliminary PEO-PEE block copolymer phase diagram are consistent with our understanding of block copolymer phase behavior with respect to the location of the complex phase window and asymmetry in the phase diagram associated with the asymmetric statistical segment lengths of PEO and PEE (*13*, *23*, *24*). The phase behavior in these materials is qualitatively similar to that of both hydrocarbon-based, higher MW block copolymers and lower MW, solvated nonionic surfactants. However, fundamental differences associated with thermoreversibility and epitaxial relations occur.

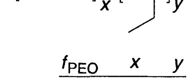

Fig. 1. The structure of PEO-PEE block copolymers. The PEE blocks contain ~10 mol % linear C_4H_8 units; f_{PEO} denotes the volume fraction of PEO.

	f_{PEO}	x	y
OE10	0.72	152	35
OE5	0.70	143	37

M. A. Hillmyer and F. S. Bates, Department of Chemical Engineering and Materials Science, University of Minnesota, Minneapolis, MN 55455, USA.
K. Almdal and K. Mortensen, Risø National Laboratory, DK-4000 Roskilde, Denmark.
A. J. Ryan, Materials Science Centre, University of Manchester Institute of Science and Technology, Manchester, M1 7HS, UK, and Daresbury Laboratory, Warrington, WA 44AD, UK.
J. P. A. Fairclough, Materials Science Centre, University of Manchester Institute of Science and Technology, Manchester, M1 7H5, UK.

*To whom correspondence should be addressed. E-mail: hillmyer@cems.umn.edu

Thermally induced order-order transitions are observed in lyotropics (*16*, *25*) and block copolymers (*20*, *26–29*) at constant water concentrations or block compositions, respectively. Epitaxial relations between phases, transition kinetics, mechanisms of transformation, and reversibility all influence the applications of these materials. We focus the remaining discussion on two of the PEO-PEE block copolymers, **OE10** and **OE5** (Fig. 1), which exhibited multiple ordered phases accessible through changes in temperature. **OE10** showed the following sequence of six phases upon heating: L_c, L, ML, $Q_{Ia\bar{3}d}$, H, and DIS. This sequence of six distinct thermotropic phases is the most reported for any block copolymer sample to the best of our knowledge. **OE5** exhibited a similar phase sequence upon heating, except the $Q_{Ia\bar{3}d}$ phase melted into the DIS phase. The appearance of the H phase in **OE10** is consistent with the larger compositional asymmetry (*13–15*).

The linear viscoelastic properties of soft materials are sensitive to changes in morphology. We identified phase-transition temperatures by measuring the dynamic elastic shear modulus (G') of **OE10** and **OE5** with a dynamic mechanical spectrometer operated at small strain ($\leq$1%) and low frequency (1 rad/s) (*30*). The temperature dependence of G' for **OE10** and **OE5** is shown in Fig. 3. The G' levels associated with the separate phases are spread over four orders of magnitude. The cooling curves show that the overall L $\leftrightarrow$ $Q_{Ia\bar{3}d}$ transition is reversible only in **OE5**. There, the $Q_{Ia\bar{3}d}$ phase can be cooled well below the ML $\rightarrow$ $Q_{Ia\bar{3}d}$ transition temperature observed on heating, and then the modulus level drops to the original L level. The reverse transition back to L appears to bypass the ML state. In **OE10**, the $Q_{Ia\bar{3}d}$ $\leftrightarrow$ H and L $\leftrightarrow$ ML transitions are reversible, but the $Q_{Ia\bar{3}d}$ $\rightarrow$ ML (or L) transition does not occur; the bicontinuous cubic state persists upon cooling until the PEO block crystallizes. These reversibility results were confirmed by small-angle scattering experiments.

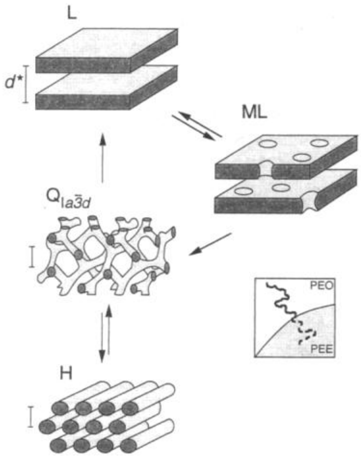

Fig. 2. The four noncrystalline ordered morphologies identified in PEO-PEE block copolymers. Arrows identify observed order-order transitions. The transition from L to $Q_{Ia\bar{3}d}$ is mediated by the ML state. An illustration of the interfacial structure is provided in the inset.

Small-angle scattering was used to determine the principal interplanar spacing, d^*, as a function of temperature for **OE10** (Fig. 4) (*31*). Heating the sample resulted in a gradual decrease in d^* and more abrupt changes at the rheologically determined phase-transition temperatures. A remarkable feature of this change in d^* with microstructure is the difference between values of d^* for the L and $Q_{Ia\bar{3}d}$ phases, which correspond to the d_{001} and d_{211} lattice spacings, respectively. Because the $Q_{Ia\bar{3}d}$ phase can be cooled to temperatures where L exists upon heating, the d^* values for the two phases can be compared directly. At 90°C, d_{001} for **OE10** is 16% greater than d_{211} (the d^* spacing for the L morphology in **OE5** is ~8% larger than that for the $Q_{Ia\bar{3}d}$ phase). In comparison, the fundamental length scale is identical at constant water composition for the L $\leftrightarrow$ $Q_{Ia\bar{3}d}$ $\leftrightarrow$ H transitions (that is, $d_{001} \cong d_{211} \cong d_{01}$) in the $C_{12}EO_6$ nonionic surfactant system (*25*, *32*). Also, in high-MW block copolymers the changes in spacing associated with changes in microstructure are experimentally observed (*26–28*, *33*) and theoretically predicted (*15*) to be small (<3%).

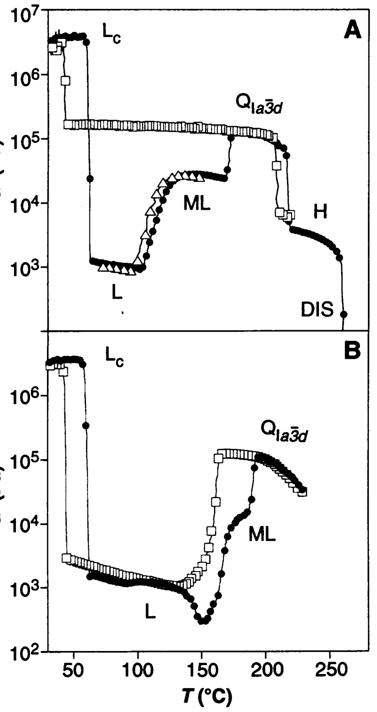

Fig. 3. Temperature dependence of the low-frequency dynamic elastic shear modulus (G') for **OE10** (**A**) and **OE5** (**B**). The samples were loaded in a shear sandwich configuration above the PEO melt temperature and annealed at 30°C for 1 hour. They were then heated under a N_2 atmosphere at 1°C/min (filled circles). Cooling curves were obtained by heating a sample into the high-temperature phase and cooling at 1°C per minute (open squares are from the H phase, and open triangles are from the ML phase). **OE5** disorders (DIS) at 242°C (not shown). Only 10% of the actual data points are shown for clarity.

A transition from the L to $Q_{Ia\bar{3}d}$ phase involves a complicated topological change from a one- to a three-dimensional structure (Fig. 2). In both **OE10** and **OE5**, an ML structure is observed between the L and the $Q_{Ia\bar{3}d}$ phases. We believe this ML intermediate phase serves as both a topological and epitaxial pathway for the L to $Q_{Ia\bar{3}d}$ transition in both **OE5** and **OE10**. Once the interplanar spacing becomes close enough to allow the transition, it occurs almost spontaneously, as evidenced by the sharp rise in G' at the ML to $Q_{Ia\bar{3}d}$ transition temperatures (Fig. 3). These results suggest that a direct transition from L to $Q_{Ia\bar{3}d}$ is not possible in these materials. However, the reverse transition can occur with no apparent intermediate, as in **OE5**. The thermoreversibility of the L $\leftrightarrow$ $Q_{Ia\bar{3}d}$ transition in **OE5** suggests that these are the equilibrium phases. In **OE10**, however, the low-temperature equilibrium phase is less obvious (*34*).

Crystallization of the PEO block in **OE10** (and in other PEO-PEE samples) disrupts the bicontinuous cubic phase, leading to extended PEO chains (two folds per PEO block in **OE10**) that can be accommodated only by a layered (L_c) morphology. The lamellar domain spacing is much larger

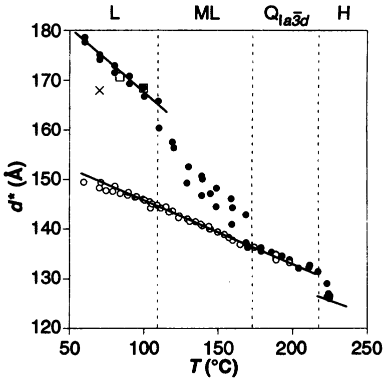

Fig. 4. Principal microstructure spacing, d^*, as a function of temperature for **OE10** determined by SANS: filled circles, heated from the L_c phase; open squares, cooled from the ML phase; open circles, cooled from the H phase; ×, spacing obtained after the application of a large amplitude shear to the cooled material. The solid lines serve as guides to the eye. The rheologically determined phase-transition temperatures are shown as dotted lines.

than the L phase ($d^*_{25°C} \cong 210$ Å, $d^*_{60°C} \cong 170$ Å). If a match in d spacing is required for the L to $Q_{Ia\bar{3}d}$ transition, an even larger mismatch will further inhibit the L_c to $Q_{Ia\bar{3}d}$ transition. We have not observed a direct transition from L_c to $Q_{Ia\bar{3}d}$ in any PEO-PEE sample. Formation of the L phase upon heating from the L_c phase occurs because the phases are topologically identical, and therefore it appears that a large spacing mismatch does not inhibit this transition.

These low-MW PEO-PEE block copolymers appear to behave as both block copolymers and lyotropic LCs, and in fact most of the phase behavior reported here has been seen in both classes of amphiphiles (*2, 13, 14, 26–29*). However, the length scale mismatch between the L and the $Q_{Ia\bar{3}d}$ phases is significantly enhanced in these polymers, and this mismatch inhibits the forward transition. These polymers highlight two important factors in soft material phase transitions: epitaxy and molecular conformation. We believe the large lattice mismatches in these polymers can be thought of as a consequence of "double frustration." Packing frustration in lyotropic systems occurs on only one side of the microdomain space because of the solvated state of the hydrophilic side (that is, water plus polar head group). The additional degree of freedom imparted by the water permits the system to accommodate a larger number of morphologies at fixed lattice spacing purely on the basis of the ability of the water to move relatively freely within the microdomain space. This freedom also appears to facilitate phase transitions. In a block copolymer melt, a single-component system, molecular conformation is "frustrated" on both sides of the microdomain space. However, increasing MW increases the number of conformational states available to the chains, and this appears to mitigate packing frustration (*14, 26*). The large number of conformational states in high-MW block copolymers seems to play the same role that water does in the lyotropic systems. Therefore, differences in domain spacing between phases are either small or nonexistent.

The PEO-PEE block copolymers described here were designed to amplify the effects of double frustration. We have enhanced the frustration on both sides of the microdomain space by removing the water normally present in solvated nonionic surfactants and by decreasing the MW found in typical block copolymers. Those changes exaggerated the effects on ordered-state phase transitions. The addition of water or homopolymer to these block copolymers will enable us to test this hypothesis and move continuously from thermotropic block copolymer phase behavior to lyotropic block copolymer phase behavior in one system.

REFERENCES AND NOTES

1. R. G. Laughlin, *The Aqueous Phase Behavior of Surfactants* (Academic Press, San Diego, 1994).
2. J. M. Seddon, *Biochim. Biophys. Acta* **1031**, 1 (1990).
3. S. M. Gruner, *J. Phys. Chem.* **93**, 7562 (1989).
4. P. Mariani, V. Luzzati, H. Delacroix, *J. Mol. Biol.* **204**, 165 (1988).
5. Y.-S. Lee *et al., J. Am. Chem. Soc.* **117**, 5573 (1995).
6. S. Puvvada, S. Baral, G. M. Chow, S. B. Qadri, B. R. Ratna, *ibid.* **116**, 2135 (1994).
7. A. Monnier *et al., Science* **261**, 1299 (1993).
8. J. S. Beck *et al., J. Am. Chem. Soc.* **114**, 10834 (1992).
9. J. Burgoyne, M. C. Holmes, G. J. T. Tiddy, *J. Phys. Chem.* **99**, 6054 (1995).
10. F. S. Bates, *Science* **251**, 898 (1991).
11. ______ and G. H. Fredrickson, *Annu. Rev. Phys. Chem.* **41**, 525 (1990).
12. S. Chandrasekhar, *Liquid Crystals* (University Press, Cambridge, 1992).
13. F. S. Bates, M. F. Schulz, A. K. Khandpur, S. Förster, J. H. Rosedale, *Faraday Discuss.* **98**, 7 (1994).
14. S. Förster *et al., Macromolecules* **27**, 6922 (1994).
15. M. W. Matsen and F. S. Bates, *ibid.*, in press.
16. J. D. Mitchell, G. J. T. Tiddy, L. Waring, T. Bostock, M. P. McDonald, *J. Chem. Soc. Faraday Trans. 1* **79**, 975 (1983).
17. K. Kratzat and H. Finkelmann, *Colloid Polym. Sci.* **272**, 400 (1994).
18. M. A. Hillmyer and F. S. Bates, in preparation.
19. The PEE block in these block copolymers is an amorphous material with a glass transition temperature of approximately −30°C.
20. I. W. Hamley *et al., Macromolecules* **26**, 5959 (1993).
21. S. S. Funari, M. C. Holmes, G. J. T. Tiddy, *J. Phys. Chem.* **98**, 3015 (1994).
22. For a complete discussion of the methods used to determine the microstructures of ordered block copolymers, see (*13, 14, 28–30*).
23. F. S. Bates and G. H. Fredrickson, *Macromolecules* **27**, 1065 (1994).
24. M. W. Matsen and M. Schick, *ibid.*, p. 4014.
25. M. Clerc, A. M. Levelut, J. F. Sadoc, *J. Phys. II (France)* **1**, 1263 (1991).
26. D. A. Hajduk *et al., Macromolecules* **27**, 490 (1994).
27. D. A. Hajduk *et al., ibid.*, p. 4063.
28. M. F. Schulz, F. S. Bates, K. Almdal, K. Mortensen, *Phys. Rev. Lett.* **73**, 86 (1994).
29. A. K. Khandupur *et al., Macromolecules* **28**, 8796 (1995).
30. J. H. Rosedale, F. S. Bates, K. Almdal, K. Mortensen, G. D. Wignall, *ibid.*, p. 1429.
31. SANS experiments were conducted at the Risø National Laboratory, Denmark, with neutrons of 5.6 Å wavelength. The SAXS experiments were conducted at the CCLRC radiation source at Daresbury, UK, with x-rays of 1.50 Å wavelength. The fundamental interplanar spacing d^* is equal to $2\pi/q^*$, where q^* is the principal scattering wave vector. Selective deuteration of the PEE block in the synthesis of **OE10** provided large neutron scattering contrast. The PEO-PEE materials have substantial x-ray contrast.
32. Y. Rançon and J. Charvolin, *J. Phys. Chem.* **92**, 2646 (1988).
33. K. A. Koppi, M. Tirrell, F. S. Bates, K. Almdal, K. Mortensen, *J. Rheol.* **38**, 999 (1994).
34. Long-time annealing experiments and temperature quenches from the DIS state lead us to believe that the equilibrium phase at low temperature in **OE10** is $Q_{Ia\bar{3}d}$. Cooperative chain stretching induced by PEO block crystallization apparently resets the system to a nonequilibrium state. Application of large amplitude shear can have the same effect. Shearing a sample that was cooled from the $Q_{Ia\bar{3}d}$ state results in a spacing that is similar to the L spacing obtained on heating from the L_c state (see Fig. 4).

35. Supported by Air Force Office of Scientific Research grant AF/F49620-93-0182 and by the Center for Interfacial Engineering, an NSF Engineering Research Center. EPSRC is acknowledged for providing x-ray beam time. F.S.B. and K.A. benefited from a NATO travel grant. We thank M. Matsen and D. Hajduk for helpful discussions during the preparation of this manuscript.

3 October 1995; accepted 8 December 1995

Chain Migration of Neuronal Precursors

Carlos Lois, Jose-Manuel García-Verdugo,
Arturo Alvarez-Buylla*

In the brain of adult mice, cells that divide in the subventricular zone of the lateral ventricle migrate up to 5 millimeters to the olfactory bulb where they differentiate into neurons. These migrating cells were found to move as chains through a well-defined pathway, the rostral migratory stream. Electron microscopic analysis of serial sections showed that these chains contained only closely apposed, elongated neuroblasts connected by membrane specializations. A second cell type, which contained glial fibrillary acidic protein, ensheathed the chains of migrating neuroblasts. Thus, during chain migration, neural precursors moved associated with each other and were not guided by radial glial or axonal fibers.

Neurons of the central nervous system of vertebrates originate in the ventricular zone (VZ) and subventricular zone (SVZ) (*1*) and from there migrate to reach their final destinations where they differentiate. Two forms of neuronal migration have been described in the developing brain (*2*): radial migration in which young neurons climb on the shafts of radial glial cells (*3–5*), and tangential migration, in which cells move parallel to the surface of the ventricles and perpendicular to the radial glial fibers (*6–11*). Tangential migration has been inferred from the dispersal of clonally related cells (*8*), from the orientation of migrating precursors (*7, 9, 10*), and from time-lapse studies of migrating cells in brain slices in vitro (*11*).

C. Lois and A. Alvarez-Buylla, Rockefeller University, 1230 York Avenue, New York, NY 10021, USA.
J.-M. García-Verdugo, Facultad de Biológicas, Universitas Valencia, Burjassot, Valencia 46100, Spain.

*To whom correspondence should be addressed.